

A Bayesian Binaural System for 3D Sound-Source Localisation

Cátia Pinho*, João Filipe Ferreira*, Pierre Bessière[†] and Jorge Dias*

*ISR — Institute of Systems and Robotics, FCT-University of Coimbra, Coimbra, Portugal

[†]CNRS-Grenoble, France

Abstract—In this text we present a Bayesian system of auditory localisation in distance, azimuth and elevation using binaural cues only. We describe its supporting sensor model and calibration procedure. The binaural system is also integrated in a spatial representation framework for multimodal perception of 3D structure and motion — the Bayesian Volumetric Map (BVM). This solution will enable the implementation of an active perception system with great potential in applications as diverse as social robots or even robotic navigation.

I. INTRODUCTION

Although vision might be the dominant sense in humans, we rely on hearing as our only panoramic, long-range sensory system. The ability not only to detect and identify a sound, but also to pinpoint swiftly and accurately the location of its source can bring substantial advantages. This applies equally to a predator stalking its prey in the wild [1] and to robotic applications such as [2], [3], [4], [5], [6], [7]. Moreover, auditory stimulus localisation is also an important component driving attention and gaze shifts, especially when the target is not in sight [6].

In this text we present a Bayesian system of auditory localisation in distance, azimuth and elevation using binaural cues only. We describe its supporting sensor model and calibration procedure. The binaural system is also integrated in a spatial representation framework for multimodal perception of 3D structure and motion, the Bayesian Volumetric Map (BVM) — for more details, please refer to [8].

To support our research work, an artificial multimodal perception system (IMPEP — Integrated Multimodal Perception Experimental Platform) has been constructed at the ISR/FCT-UC consisting of a stereovision, binaural and inertial measuring unit (IMU) setup mounted on a motorised head, with gaze control capabilities for image stabilisation and perceptual attention purposes — see Fig. 1. This solution will enable the implementation of an active perception system with great potential in applications as diverse as social robots or even robotic navigation (Fig. 2).

The *Bayesian Program* (BP) formalism, as first defined by Lebeltel [9], will be used to define the sensor model presented herewith.

II. BAYESIAN BINAURAL SENSOR MODEL

The Bayesian binaural system presented herewith is composed of three distinct and consecutive processors (Fig. 3):

This publication has been supported by EC-contract number FP6-IST-027140, Action line: Cognitive Systems. The contents of this text reflect only the author's views. The European Community is not liable for any use that may be made of the information contained herein.

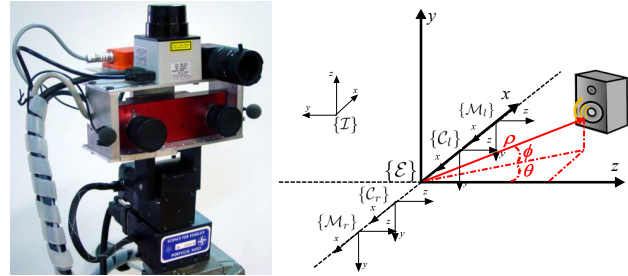


Fig. 1. View of the current version of the Integrated Multimodal Perception Experimental Platform (IMPEP), on the left. On the right, the IMPEP perceptual geometry is shown: $\{\mathcal{E}\}$ is the main reference frame for the IMPEP robotic head, representing the egocentric coordinate system; $\{C_{l,r}\}$ are the stereovision (respectively left and right) camera referentials; $\{M_{l,r}\}$ are the binaural system (respectively left and right) microphone referentials; and finally $\{\mathcal{I}\}$ is the inertial measuring unit's coordinate system.



Fig. 2. Typical application context of the IMPEP active perception system.

the *monaural cochlear unit*, which processes the pair of monaural signals $\{x_1, x_2\}$ coming from the binaural audio transducer system by simulating the human cochlea, so as to achieve a *tonotopic* representation (i.e. a frequency band decomposition) of the left and right audio streams; the *binaural unit*, which correlates these signals and consequently estimates the binaural cues and segments each sound-source; and, finally, the *Bayesian 3D sound-source localisation unit*, which applies a Bayesian sensor model so as to perform localisation of sound-sources in 3D space.

A. Cochlear and auditory periphery processing

The first stages of auditory processing consist of cochlear and auditory periphery processing, which produces what is called an *auditory image model* (AIM) [10]. The AIM processor implements a functional model of a cochlea that

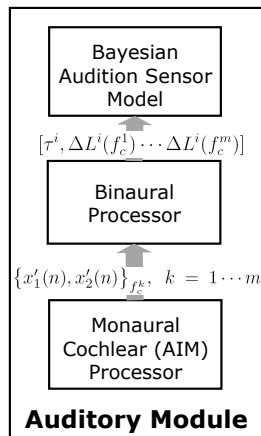


Fig. 3. The IMPEP Bayesian binaural system.

simulates the phase-locked activity that complex sounds produce in the auditory nerve.

Spectral analysis, the first stage of the AIM, is performed by a bank of auditory filters which converts each digitised wave that composes the stereo signal into an array of filtered waves. This processing is done using *gammatone filters* [11], [12], linearly distributed along a frequency scale measured in *equivalent rectangular bandwidths* (ERBs), as defined by [13] for simulating the cochlea, obtaining a model of *basilar membrane motion* (BMM) through frequency band decomposition.

The second stage of the AIM simulates the mechanical/neural transduction process performed by the inner hair-cells. It converts the BMM into a *neural activity pattern* (NAP), which is the AIM’s representation of the afferent activity in the auditory nerve [10]. In this stage the envelopes of the signals are first compressed, and then subjected to halfwave rectification followed by a squaring and lowpass filtering, resulting in m stereo audio signal pairs corresponding to m frequency channels with respective frequency centre f_c^k , $\{x'_1(n), x'_2(n)\}_{f_c^k}$, $k = 1 \dots m$.

B. Binaural cue processing

Sound waves arising from a source on our left will arrive at the left ear first. This small, but perceptible, difference in arrival time (known as an ITD, interaural time difference) is an important localisation cue and is detected by the *inferior colliculus* in primates, which acts as a temporal correlation detector array, after the auditory signals have been processed by the cochlea. Similarly, for intensity, the far ear lies in the head’s “sound shadow”, giving rise to interaural level differences (ILDs) [1], [14]. ITDs vary systematically with the angle of incidence of the sound wave relative to the interaural axis, and are virtually independent of frequency, representing the most important localisation cue for low frequency signals (< 1500 Hz in humans). ILDs are more complex than ITDs in that they vary much more with sound frequency. Low-frequency sounds easily travel around the head and produce negligible ILDs. ILD values produced at

higher frequencies are larger, and are increasingly influenced by the filter properties of each external ear, which imposes peaks and notches on the sound spectrum reaching the eardrum. Instead of being centred on the interaural axis, cones of confusion associated with particular ILD values take a different shape for each sound frequency.

Moreover, when considering sound sources within 1 – 2 meters of the listener, binaural cues alone can even be used to fully localise the source in 3D space (i.e. azimuth, elevation and distance). Iso-ITD surfaces form hollow cones of confusion with a specific thickness extending from each ear in a symmetrical configuration relatively to the medial plane. On the contrary, iso-ILD surfaces, which are spherical surfaces delimit hollow spherical volumes, symmetrically placed about the medial plane and centred on a point on the interaural axis [15]. Thus, for sources within 2 meters range, the intersection of the ILD and ITD volumes is a torus-shaped volume [15]. If the source is more than 2 meters away, the change in ILD with source position is too gradual to provide spatial information (at least for an acoustically transparent head), and the source can only be localised to a volume around the correct cone of confusion [15].

Given this background, we have decided to adapt the solution by Faller and Merimaa [16] to implement the binaural processor. Using this algorithm, interaural time difference and interaural level difference cues are only considered at time instants when only the direct sound of a specific source has nonnegligible energy in the critical band and, thus, when the evoked ITD and ILD represent the direction of that source (corresponding to the process involving the *superior olivary complex* (SOC) and the *central nucleus of the inferior colliculus* (ICc) in mammals). They show how to identify such time instants as a function of the *interaural coherence* (IC). The source localisation suggested by the selected ITD and ILD cues are shown to imply the results of a number of published psychophysical studies related to source localisation in the presence of distractors, as well as in precedence effect conditions [17]. This algorithm thus amplifies the signal-to-noise ratio and facilitates auditory scene analysis for multiple auditory object tracking, and is briefly summarised in the following paragraphs — for more details, please refer to [16].

The ITD and IC, denoted respectively by $\tau(n)$ and $c_{12}(n)$, where n indexes the sample currently being processed, are estimated from the normalised cross-correlation functions of the signals from left and right ear for each centre frequency f_c , respectively x'_1 and x'_2 . The normalisation of the cross-correlation function is introduced in order to get an estimate of the IC, defined as the maximum value of the instantaneous normalised cross-correlation function. This estimate describes the coherence of the left and right ear input signals. In principle, it has a range of $[0; 1]$, where 1 occurs for perfectly coherent x'_1 and x'_2 . However, due to the DC offset of the halfwave rectified signals, the values of c_{12} are typically higher than 0 even for independent (nonzero) x'_1 and x'_2 . Thus, the effective range of the interaural coherence c_{12} is compressed to $[a; 1]$ by the neural transduction. The

compression is more pronounced (larger a) at high frequencies, where the low pass filtering of the half-wave rectified critical band signals yields signal envelopes with a higher DC offset than in the signal wave forms [16].

The ILD, denoted as $\Delta L(n)$, is then computed using the signal levels at the corresponding offsets [16]. Note that due to the envelope compression the resulting ILD estimates will be smaller than the level differences between the ear input signals. For coherent ear input signals with a constant level difference, the estimated ILD (in dB) will be 0.23 times that of the physical signals [16].

When several independent sources are concurrently active in free field, the resulting cue triplets $\{\Delta L(n), \tau(n), c_{12}(n)\}$ can be classified into two groups [16]: (1) Cues arising at time instants when only one of the sources has power in that critical band. These cues are similar to the free-field cues — localisation is represented in $\{\Delta L(n), \tau(n)\}$, and $c_{12}(n) \approx 1$. (2) Cues arising when multiple sources have non-negligible power in a critical band. In such a case, the pair $\{\Delta L(n), \tau(n)\}$ does not represent the direction of any single source, unless the superposition of the source signals at the ears of the listener incidentally produces similar cues. Furthermore, when the two sources are assumed to be independent, the cues are fluctuating and $c_{12}(n) < 1$. These considerations motivate the following method for selecting ITD and ILD cues. Given the set of all cue pairs, $\{\Delta L(n), \tau(n)\}$, only the subset of pairs is considered which occurs simultaneously with an IC larger than a certain threshold, $c_{12}(n) > c_0$. This subset is denoted

$$\{\Delta L(n), \tau(n) | c_{12}(n) > c_0\} \quad (1)$$

The same cue selection method is applicable for deriving the direction of a source while suppressing the directions of one or more reflections. When the “first wave front” arrives at the ears of a listener, the evoked ITD and ILD cues are similar to the free-field cues of the source, and $c_{12}(n) \approx 1$. As soon as the first reflection from a different direction arrives, the superposition of the source signal and the reflection results in cues that do not resemble the free-field cues of either the source or the reflection. At the same time IC reduces to $c_{12}(n) < 1$, since the direct sound and the reflection superimpose as two signal pairs with different ITD and ILD. Thus, IC can be used as an indicator for whether ITD and ILD cues are similar to free-field cues of sources or not, while ignoring cues related to reflections.

Faller and Merimaa’s cue selection method, as the authors point out, can be seen as a “multiple looks” approach for localisation, which provides the motivation for our implementation. Multiple looks have been previously proposed to explain monaural detection and discrimination performance with increasing signal duration [18]. The idea is that the auditory system has a short-term memory of “looks” at the signal, which can be accessed and processed selectively. In the context of localisation, the looks would consist of momentary ITD, ILD, and IC cues. With an overview of a set of recent cues, ITDs and ILDs corresponding to high IC

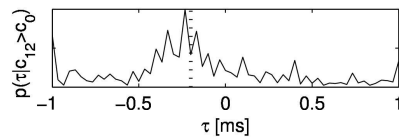


Fig. 4. Example of the use of an adaptation of the cue selection method proposed by [16] using a 1 s “multiple looks” buffer. Represented in the figure is a histogram of collected ITD cues corresponding to high IC levels for a particular frequency channel of a 1 s audio snippet. This histogram is interpreted as a distribution corresponding to the probability of the occurrence of ITD readings, which is then used as a conspicuity map in order to perform a *summary cross-correlogram* over all frequencies (see main text for more details).

values are adaptively selected and used to build a histogram that provides a statistical description of gathered cues (see Fig. 4).

Finally, the binaural processor capitalises on the multiple looks configuration and implements a simple auditory scene analysis algorithm for detection and extraction of important auditory features to build conspicuity maps and ultimately a saliency map, thus providing a functionality similar to the role of the *external nucleus of the inferior colliculus* (ICx) in the mammalian brain. The first stage of this algorithm deals with figure-ground (i.e. foreground-background) segregation and signal-to-noise ratio. In signal processing, the energy of a discrete-time signal $x(n)$ is given by [19]

$$E = \sum_{-\infty}^{\infty} |x(n)|^2$$

Using this notion, a simple strategy can be followed to selectively apply the multiple looks approach to a binaural audio signal buffer so that only relevant audio snippets are analysed. This strategy goes as follows: given a binaural signal buffer of N samples represented by the tuple $\{x'_1(n), x'_2(n)\}$, the average of the energies of the component signals $x'_1(n)$ and $x'_2(n)$ is

$$E_{avg} = \frac{\sum_1^N |x'_1(n)|^2 + \sum_1^N |x'_2(n)|^2}{2} \quad (2)$$

and can be used as a noise gate so that only when $E_{avg} > E_0$ ITDs, ILDs and ICs triplets are collected for the buffer, yielding multiple looks values only for relevant signals (just the ITD-ILD pairs corresponding to high IC values are kept in conspicuity maps per frequency channel), while every other buffer instantiation is labelled as irrelevant noise. E_0 can be fixed to a reasonable empirical value or be adaptive, as seems to happen with human hearing. A set of results exemplifying this algorithm is presented on Fig 5.

Once the multiple looks information is gathered, since ITDs are proven to be stable across frequencies for a specific sound source at a given azimuth regardless of range or elevation, the ITD conspicuity maps may be summed over all frequencies, in a process similar to what is believed to occur in the ICx, in computational terms known as a *summary cross-correlogram* (again see Fig. 4). From the resulting one-dimensional signal, the largest peaks may be

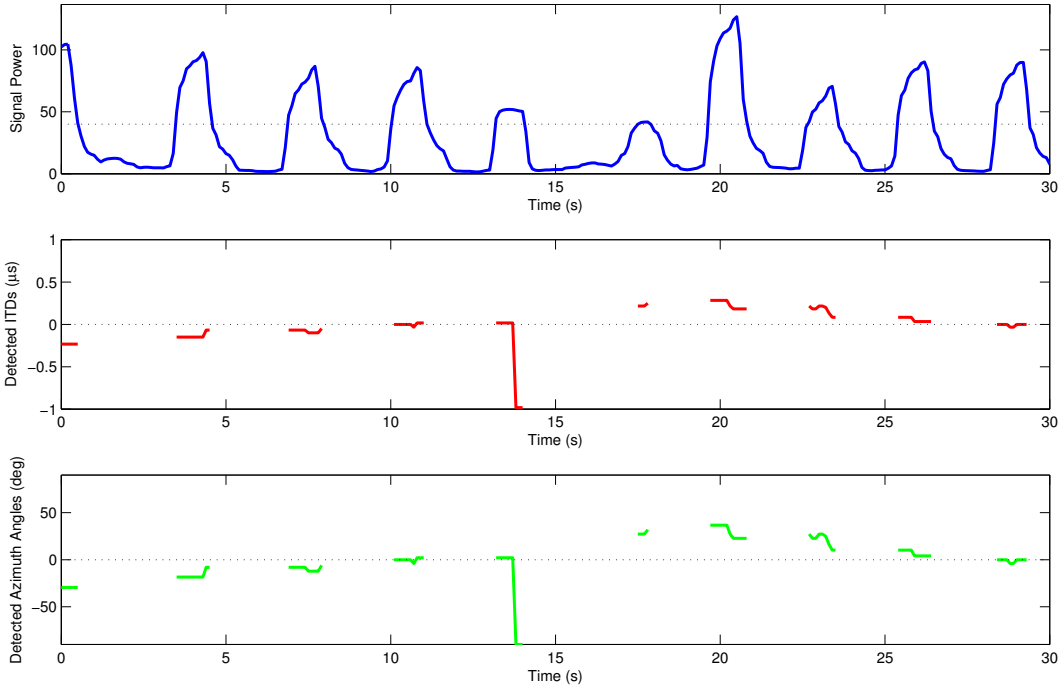


Fig. 5. Binaural processing results of an approximately 30 second-long audio snippet of a typical “cocktail party” scenario, with the main voice calling out “Nicole, look at me”, while other voices can be heard coming from sites close to the robotic head, elsewhere in the lab. The active perception head was moved while the main voice speaker was kept still, first keeping the speaker to the right and slowly travelling towards the centre, then keeping the speaker to the left and again slowly moving towards the centre. Top — the effect of the signal power-based figure-ground segregation noise gate is shown (dashed line represents gate threshold); Middle — ITD estimates for the most salient sound; Bottom — corresponding azimuth estimates. These results show the performance of the binaural processor under difficult conditions, the only “failure” being the estimates corresponding to the 14 s instant: for a signal power above the interest threshold, the background noise (i.e., some other voice in the lab) was more salient than the main voice.

taken as having been effected by the most important sound-sources represented in the auditory image. Then, a search is made across each frequency band to find the closest ITD and its ILD pair, for each reference ITD, thus building n -sized vectors (for $m = n - 1$ frequency channels) for each relevant sound source of the form

$$A = [\tau, \Delta L(f_c^1) \cdots \Delta L(f_c^m)] \quad (3)$$

C. Bayesian sensor model

Finally, regarding the Bayesian 3D sound-source localisation unit, auditory sensor space is defined as a log-spherical volumetric occupancy grid \mathcal{Y}' , with each cell being indexed by its far corner $C \equiv (\log_{b'} \rho_{\max}, \theta_{\max}, \phi_{\max}) \in C' \subset \mathcal{Y}'$ — this configuration follows the same formalism as the Bayesian Volumetric Map (BVM) framework, described in [8].

The set of cell indices C' in auditory space is a subset of cell indices \mathcal{C} in BVM space, and thus the indexing used for the auditory sensor space \mathcal{Y}' also corresponds to cells in the BVM space \mathcal{Y} ; however, different resolutions are assumed to accommodate the difference between visual and auditory accuracy ratings. Hence the need of a related base for log-space given by $b' = a^{k \log_a b}, \forall a \in \mathbb{R}$. This relation ensures that log-space in the auditory sensor spatial domain and log-space in the BVM are related by factor k , in the sense that one cell in b' log-space corresponds to k cells in b log-space. Consequently, the important spatial relation $C' = \bigcup_{i=1}^N \mathcal{C}$ is

also ensured through the additional relations $\Delta\theta' = i \times \Delta\theta$ and $\Delta\phi' = j \times \Delta\phi$ and allows measurements from one cell in auditory space to precisely correspond to $N = i \times j \times k$ cells in the BVM (for more details please refer to [8]).

The direct audition sensor model is formulated as the first question of the Bayesian Program in Fig. 6, where all relevant variables and distributions and the decomposition of the corresponding joint distribution, according to Bayes’ rule and dependency assumptions, are defined. The use of the auxiliary binary random variable S_C , which signals the presence or absence of a sound-source in cell C , and the corresponding family of probability distributions $P(S_C | O_C C) \equiv P(S_C | O_C)$ promotes the assignment of probabilities of occupancy close to 1 for cells for which the binaural cue readings seem to indicate a presence of a sound-source and close to .5 otherwise (i.e. the absence of a detected sound-source in a cell doesn’t mean that the cell is empty). The family of distributions is given in tabular fashion: obviously, $P([S_C = 1] | [O_C = 0]) = 0$ and $P([S_C = 0] | [O_C = 0]) = 1$, while $P([S_C = 1] | [O_C = 1]) = P_{SS}$ and $P([S_C = 0] | [O_C = 1]) = 1 - P_{SS}$ are dependent on the probability assigned to an occupied cell corresponding to the position of a sound-source, denoted by P_{SS} , which can be empirically chosen or statistically learned through the analysis of several typical perceptual scenarios.

The second question corresponds to the estimation of the position of cells most probably occupied by sound sources,

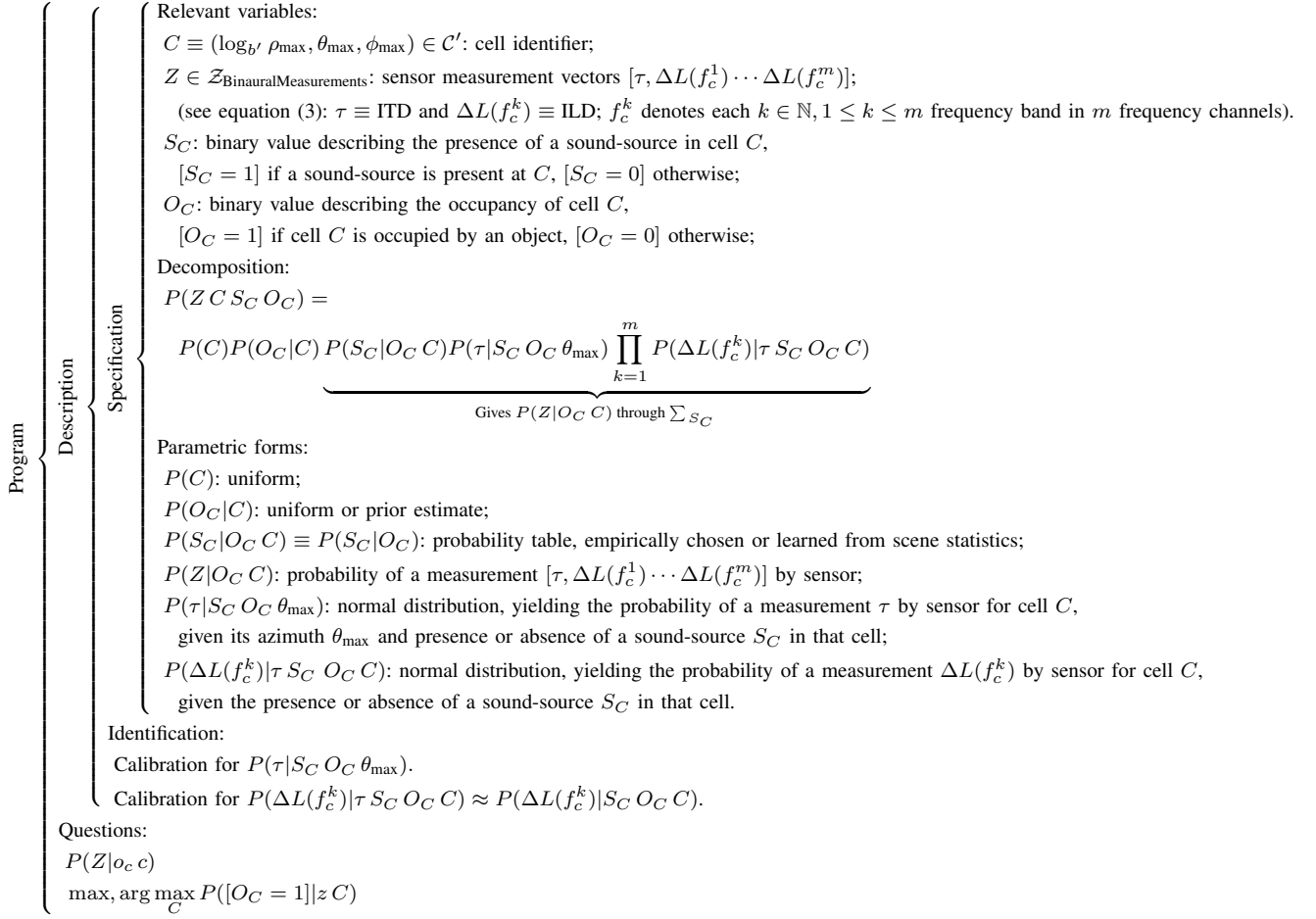


Fig. 6. Bayesian Program for binaural sensor model.

through the inversion of the direct model through Bayesian inference on the joint distribution decomposition equation. The former is used as a sub-BP for the BVM, while the answer to the latter yields a gaze direction of interest in terms of auditory features for the multimodal attention system, using a maximum *a posteriori* (MAP) method.

III. BAYESIAN BINAURAL SYSTEM CALIBRATION

As can be seen on the BP in Fig. 6, calibration of the binaural system involves the characterisation of the families of normal distributions $P(\tau|S_C O_C \theta_{\max})$ and $P(\Delta L(f_c^k)|\tau S_C O_C C) \approx P(\Delta L(f_c^k)|S_C O_C C)$ through descriptive statistical learning of their central tendency and statistical variability. This is done in an equivalent manner as with commonly used head-related transfer function (HRTF) calibration processes (see, for example, [20]) and is described in the following paragraphs.

A set M_C of n -dimensional measurement vectors such as defined in equation (3) is consequently collected per cell $C \in \mathcal{C}'$. The full set of collected measurement vectors for all cells in auditory sensor space \mathcal{Y}' is expressed as $M = \bigcup M_C$. Denoting $M_{\bar{C}} = M \setminus M_C$ as the set of measurements for all cells other than C , the statistical characterisation process of each family of distributions is effected through

$$P(\tau|[S_C = 1] O_C \theta_{\max}) \equiv \mathcal{N}(\tau, \mu_{\tau}(M_C), \sigma_{\tau}(M_C)) \quad (4a)$$

$$P(\tau|[S_C = 0] O_C \theta_{\max}) \equiv \mathcal{N}(\tau, \mu_{\tau}(M_{\bar{C}}), \sigma_{\tau}(M_{\bar{C}})) \quad (4b)$$

$$P(\Delta L(f_c^k)|[S_C = 1] O_C C) \equiv \mathcal{N}(\Delta L(f_c^k), \mu_{\Delta L(f_c^k)}(M_C), \sigma_{\Delta L(f_c^k)}(M_C)) \quad (4c)$$

$$P(\Delta L(f_c^k)|[S_C = 0] O_C C) \equiv \mathcal{N}(\Delta L(f_c^k), \mu_{\Delta L(f_c^k)}(M_{\bar{C}}), \sigma_{\Delta L(f_c^k)}(M_{\bar{C}})) \quad (4d)$$

Auditory calibration is performed by presenting a broadband audio stimulus through a loudspeaker positioned in well-known spatial coordinates corresponding to the geometric centre of each cell $C \in \mathcal{C}'$ so as to sample space according to the auditory sensor space \mathcal{Y}' . The experimental setup used for this purpose is described in Fig. 7.

The acquisition method may be simplified by a factor of 4 by taking into account the spatial redundancies of auditory sensing, namely the symmetry enforced by the back-to-front ambiguity and the left-to-right antisymmetry for both ITDs and ILDs, to reduce calibration space to the front-left quadrant.

A further simplification of the procedure consists in positioning the loudspeaker, for each of the N_d considered distances from the binaural system, precisely in front of

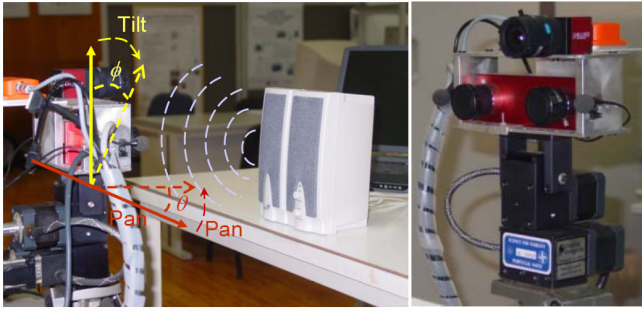


Fig. 7. Experimental setup for the binaural system calibration procedure.

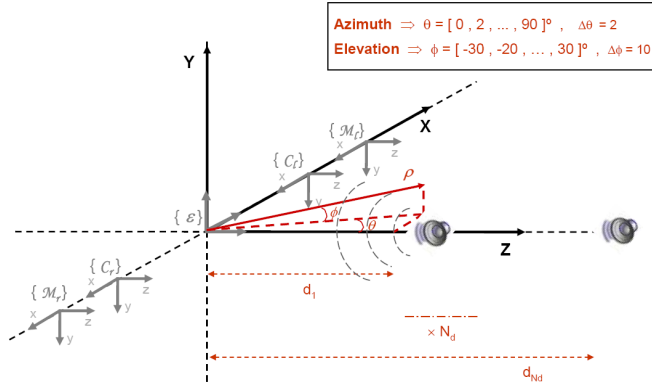


Fig. 8. Schematic of the experimental acquisition method of the auditory calibration procedure. A typical auditory sensor space is depicted, roughly based both on known human auditory precision ratings [20] and the specifications of the pan and tilt unit model PTU-46-17.5 from Directed Perception, characterised by an azimuthal range of $[0^\circ; 90^\circ]$ with $\Delta\theta = 2^\circ$ resolution and an elevation range of $[-30^\circ; 30^\circ]$ with $\Delta\phi = 10^\circ$ resolution, and a number of partitions $N = 4$, of which only the furthest $N_d = 2$ partitions would be used — the number of cells to sample amount to $[(90/2) \times (60/10) \times 2] = 540$. Thus, for 20 readings of a 1 s broadband stimulus per cell and approximately 1 s to set up each position for the loudspeaker, calibration would take about $10800 \times 2 \text{ s} = 6 \text{ h}$. This procedure allows partitioning calibration into one session per loudspeaker distance, in this case of $\approx 3 \text{ h}$.

the active perception head (i.e. $(\theta, \phi) = (0, 0)$) and to rotate the active head so that the whole range of azimuths and elevations of the auditory sensor space is covered. This replaces the several minutes taken to reposition the loudspeaker by hand (now only happening N_d times) by a few seconds of head motions for each cell. The full procedure is depicted in Fig. 8 for a typical calibration context.

IV. CONCLUSIONS

Full 3D auditory localisation has rarely been explored in robotic applications (see, for example, [20] for a review on this subject); this work contributes with a novel probabilistic solution that produces localisation estimates based on binaural cues yielded by a robust binaural processing unit. This solution has been designed so as to provide a sensor model to be used by a multimodal perception framework, the Bayesian Volumetric Map, described in [8]. Further details on the implementation of these models can be found at <http://paloma.isr.uc.pt/~jfilipe/>

BayesianMultimodalPerception.

REFERENCES

- [1] A. J. King, J. W. Schnupp, and T. P. Doubell, "The shape of ears to come: dynamic coding of auditory space," *TRENDS in Cognitive Sciences*, vol. 5, no. 6, pp. 261–270, 2001.
- [2] H. G. Okuno, K. Nakadai, T. Lourens, and H. Kitano, "Sound and Visual Tracking for Humanoid Robot," in *Proc. of 17th International Conference on Industrial and Engineering Applications of Artificial Intelligence and Expert Systems (IEA/AIE-2001)*, no. 2070. Budapest, Hungary: Springer-Verlag, June 2001, pp. 640–650.
- [3] C. Schauer and H.-M. Gross, "A Computational Model of Early Auditory-Visual Integration," in *Proceedings of the 25th Pattern Recognition Symposium (DAGM 2003)*, Magdeburg, 2003, pp. 362–369, lecture Notes in Computer Science 2781, Springer Verlag.
- [4] S. B. Andersson, A. A. Handzel, V. Shah, and P. Krishnaprasad, "Robot Phonotaxis with Dynamic Sound-source Localization," in *ICRA*, 2004.
- [5] J. Hörnstein, M. Lopes, J. Santos-Victor, and F. Lacerda, "Sound localization for humanoid robots - building audio-motor maps based on the HRTF," in *IEEE/RSJ International Conference on Intelligent Robots and Systems*, Beijing, China, October 2006.
- [6] A. Koene, J. Morén, V. Trifa, and G. Cheng, "Gaze shift reflex in a humanoid active vision system," in *5th International Conference on Computer Vision Systems (ICVS 2007)*. Bielefeld University, Germany: Applied Computer Science Group, 2007, ISBN 978-3-00-020933-8.
- [7] T. Rodemann, K. Karova, F. Joubelin, and C. Goerick, "Purely Auditory Online-Adaptation of Auditory-Motor Maps," in *2007 IEEE/RSJ International Conference on Intelligent Robots and Systems*, San Diego, CA, USA, Oct 19 – Nov 9 2007.
- [8] J. F. Ferreira, P. Bessière, K. Mekhnacha, J. Lobo, J. Dias, and C. Laugier, "Bayesian Models for Multimodal Perception of 3D Structure and Motion," in *International Conference on Cognitive Systems (CogSys 2008)*, University of Karlsruhe, Karlsruhe, Germany, April 2008.
- [9] O. Lebellet, "Programmation Bayésienne des Robots," Ph.D. dissertation, Institut National Polytechnique de Grenoble, Grenoble, France, September 1999.
- [10] R. D. Patterson, M. H. Allerhand, and C. Giguère, "Time-domain modeling of peripheral auditory processing: A modular architecture and a software platform," *J. Acoust. Soc. Am*, pp. 1890–1894, 1995.
- [11] E. de Boer, "Synthetic whole-nerve action potentials for the cat," *Acoustical Society of America Journal*, vol. 58, pp. 1030–1045, Nov. 1975.
- [12] L. V. Immerseel and S. Peeters, "Digital implementation of linear gammatone filters: Comparison of design methods," *Acoustics Research Letters Online*, vol. 4, no. 3, pp. 59–64, July 2003, Published online by the Acoustical Society of America.
- [13] R. D. Patterson, J. Holdsworth, I. Nimmo-Smith, and Rice, "SVOS Final Report: The auditory filterbank," MRC Applied Psychology Unit, Cambridge., Tech. Rep. 2341, 1988.
- [14] B. Kapralos, M. R. M. Jenkin, and E. Milios, "Auditory Perception and Spatial (3D) Auditory Systems'," York University, Tech. Rep. CS-2003-07, July 2003.
- [15] B. G. Shinn-Cunningham, S. Santarelli, and N. Kopco, "Tori of confusion: Binaural localization cues for sources within reach of a listener," *Journal of the Acoustical Society of America*, vol. 107, no. 3, pp. 1627–1636, March 2000.
- [16] C. Faller and J. Merimaa, "Source localization in complex listening situations: Selection of binaural cues based on interaural coherence," *Journal of the Acoustical Society of America*, vol. 116, no. 5, pp. 3075–3089, November 2004.
- [17] P. M. Zurek, "The precedence effect," in *Directional Hearing*, W. Yost and G. Gourevitch, Eds. Sprigler-Verlag, 1987.
- [18] N. F. Viemeister and G. H. Wakefield, "Temporal integration and multiple looks," *The Journal of the Acoustical Society of America*, vol. 90, no. 2, pp. 858–865, August 1991.
- [19] A. V. Oppenheim and R. Schaffer, *Discrete-Time Signal Processing*, N. P.-H. E. Cliffs), Ed., 1989.
- [20] P. T. Calamia, "Three-dimensional localization of a close-range acoustic source using binaural cues," Master's thesis, Faculty of the Graduate School of The University of Texas at Austin, 1998.